Conformational Analysis of a Toxic Peptide from *Trimeresurus wagleri* which Blocks the Nicotinic Acetylcholine Receptor

L. C. Sellin,* K. Mattila,* A. Annila,§ J. J. Schmidt,¶ J. J. McArdle,‖ M. Hyvönen,* T. T. Rantala,‡ and T. Kivistö*
*Divisions of Biophysics and ‡Physics, Department of Physical Sciences, University of Oulu, 90570 Oulu, Finland; §Chemical Technology, State Technical Research Centre of Finland (VTT), Biologinkuja 7, 02150 Espoo, Finland; ¶Toxinology Division, U.S. Army Medical Research Institute of Infectious Diseases, Fort Detrick, Frederick, Maryland 21702 USA; and ‖Department of Pharmacology and Toxicology, New Jersey Medical School (UMDNJ), Newark, New Jersey 07103-2714 USA

ABSTRACT The 22-residue toxic peptide (WTX1) from the venom of the Southeast Asian snake *Trimeresurus wagleri* has multiple sites of action, but its lethal effect has been attributed to blocking the postsynaptic acetylcholine receptor at the neuromuscular junction. The 3-dimensional structure of WTX1 was studied using 2-dimensional nuclear magnetic resonance spectroscopy, circular dichroism, and computer simulations. In aqueous solution, WTX1 was shown to have extended and flexible "tails" defined by a short, rigid disulfide-bonded loop. The flexible regions can undergo structural rearrangement when moved from an aqueous to a less polar environment and may contribute to its effectiveness at different receptor sites. By substituting Gly or Phe for His at position 10, significant effects on the disulfide bond formation and, thereby, the activity of the peptide were observed. These results suggest that even subtle differences in single residues can have profound effects on the dynamics of folding, disulfide bond formation, and activity of this toxic peptide.

INTRODUCTION

Trimeresurus (*Tropidolaemus*; Brattstrom, 1964) *wagleri* (Leviton, 1964) is an arboreal crotaline that ranges throughout Malaysia, the Philippines, Thailand, and the Indo-Australian archipelago to Indonesia. Previous investigations have demonstrated the presence of four lethal peptides in venom from this species (Weinstein et al., 1991; Schmidt et al., 1992). These peptides exhibit marked thermostability and highly basic isoelectric points. They contain 22–24 residues, unusually high proline content (almost 33%), and one intramolecular disulfide bond, which forms spontaneously at alkaline pH. These toxins lack phospholipase A, proteolytic, and hemolytic activity. Mice injected with lethal doses quickly develop neuromuscular paralysis.

```
                    S---S
                    |   |
WTX1      GGKPDLRPCHPPCHYIPRPKPR

                    S---S
                    |   |
WTX2      GGKPDLRPCYPPCHYIPRPKPR

                    S---S
                    |   |
WTX3    SLGGKPDLRPCHPPCHYIPRPKPR

                    S---S
                    |   |
WTX4    SLGGKPDLRPCYPPCHYIPRPKPR
```

The peptides WTX1, WTX2, and WTX3 (also known as waglerins or peptides I and II, SLPI) were synthesized, and the products were demonstrated to be the chemical and biological equivalents of the purified natural toxins (mouse i.p. LD_{50} of WTX1, WTX2, and WTX3 are 0.37, 0.58, and 0.22 mg/kg, respectively; Weinstein et al., 1991; Schmidt et al., 1992). Thus, the replacement of a single histidine residue at position 10 with tyrosine significantly reduces toxicity. Also, the reduced form of synthetic WTX1 is still toxic after i.p. injection into mice even without prior incubation at alkaline pH, which promotes disulfide bond formation. However, if one or both of the cysteine residues are replaced by serine, nontoxic peptides are produced. In addition, chymotryptic cleavage of WTX1 between residues 15 and 16 produced two nontoxic products (Schmidt et al., 1992).

Another interesting feature is that WTX1 has multiple, yet selective, sites of action. WTX1 has a curare-like action at the mammalian neuromuscular junction channels (Aiken et al., 1992; McArdle et al., 1995). To a lesser extent, it decreases transmitter release, probably through an action on presynaptic N-type Ca^{2+} channels (Aiken et al., 1992). WTX1 blocked the slow inward Ca^{2+} current in single cardiac myocytes but did not affect potassium currents (McArdle et al., 1992). In experiments using acutely dissociated hypothalamic neurons, WTX1 enhanced $GABA_A$- and glycine-activated currents (EC-50 of approximately 23 μM) but had no effect on kainate-induced currents (Ye and McArdle, 1995).

The aims of this study were to deduce the likely 3-dimensional structure of WTX1 in aqueous solution and examine the effects of single amino acid substitutions on disulfide bond formation. Preliminary reports of these findings have been published (Hyvönen et al., 1994; Mattila et al., 1995).

Received for publication 9 March 1995 and in final form 18 September 1995.
Address reprint requests to Dr. L. C. Sellin, Division of Biophysics Department of Physical Sciences, University of Oulu, 90570 Oulu, Finland. Tel.: 358-81-553-1011; Fax: 358-81-553-1101; E-mail: lawrence@phoenix.oulu.fi.

0006-3495/96/01/03/11 $2.00

MATERIALS AND METHODS

Peptides

Native WTX1 was purified as described previously (Weinstein et al., 1991; Schmidt et al., 1992). The WTX1 analogs with single amino acid substitutions at position 10, Gly10 and Phe10, were purchased from Quality Controlled Biochemicals (Hopkinton, MA) and were shown to be >98% pure by the high-pressure liquid chromatography (HPLC) data provided by the company. Further analyses were done to verify the structure and purity of the analogs, which are described in the Results. The i.p. LD_{50} of each peptide was determined by injecting Swiss-Webster mice (15–20 g) in three to five groups of four mice each as previously described (Weinstein et al., 1991).

Nerve-muscle preparations

To evaluate the neuromuscular blocking action of WTX1, two series of experiments were performed using isolated nerve-muscle preparations. In the first series, end-plate potentials (EPPs) were recorded with conventional intracellular recording techniques (Argentieri et al., 1992). To achieve this, the soleus and triangularis sterni nerve-muscle preparations were isolated from ether-anesthetized adult mice, pinned to the bottom of a Sylgard-lined plexiglass chamber, and superfused with an oxygenated (95% O_2/5% CO_2; pH 7.3–7.4) physiological solution containing (mM): NaCl 135, KCl 5 or 2.5 (crushed fiber preparation), $MgCl_2$ 1, $NaHCO_3$ 15, Na_2HPO_4 1, $CaCl_2$ 2, D-glucose 11. To block muscle twitches in response to nerve stimulation, the muscle was crushed on both sides of the end-plate region (McArdle, 1975). In the second series of experiments, the effect of WTX1 on the response of the motor end plate to iontophorectically applied acetylcholine was assayed. These measurements were made for the triangularis sterni muscle of the mouse as described previously (McArdle et al., 1981). All electrophysiological recordings were made at 21–23°C before and during exposure of the preparation to WTX1 applied via a superfusion tube with a 1-mm orifice located 50–100 μm from the target end-plate. This tube focused the flow of five needles, which were carefully aligned and glued together. These needles were connected to separate reservoirs containing various control and experimental solutions. By manually opening and closing valves, the flow of various WTX1-containing solutions could be hydrostatically controlled and provided rapid solution switching.

High-pressure liquid chromatography

HPLC of peptides was done with equipment from Waters Associates (Milford, MA). The column was an RP318 (C18), 0.46 × 25 cm, from BioRad Laboratories (Richmond, CA). Solvent A was 0.09% trifluoroacetic acid (TFA) and solvent B was 0.09% TFA/70% acetonitrile. Column temperature was maintained at 30°C and the flow rate was 1.0 ml/min. Optical density of the column effluent was monitored at 210 nm.

Amino acid sequencing

Peptides were alkylated with recrystallized iodoacetamide (without prior reduction) and then placed in a model 470A amino acid sequencer from Applied Biosystems (Foster City, CA). PTH derivatives from the sequencer were identified with a model 120A HPLC from the same manufacturer.

Disulfide bond formation

WTX1 or the analogs Phe10 and Gly10 were dissolved in 0.1% TFA at about 1 mg/ml. The pH was adjusted to 8.3 with Tris buffer, and the solution was allowed to stand at room temperature with occasional mixing. The reaction was stopped by adjusting the pH to 2.0–2.5 with TFA. Samples were kept frozen until analysis by HPLC. The presence of sulfhydryl groups was detected by reaction of an aliquot of the peptide with 5,5′-dithiobis-2-nitrobenzoic acid. Disulfide bond formation was indicated by diminution of the parent molecule HPLC peak and the appearance of a new, symmetrical HPLC peak with retention time lower than the parent molecule, and which no longer contained sulfhydryl groups.

Circular dichroism

For circular dichroism (CD) measurements, WTX3 was dissolved in trifluoroethanol (TFE) and water mixtures. The spectra were recorded at 21°C with a Jasco-720 spectrophotometer. Each scan spanned an interval from 250 nm to 190 nm taken over a 3-min period with 1-nm step resolution. The light path of the 300-μl cell was 1 mm.

NMR

NMR measurements of WTX1 and its analogs were carried out with a 600-MHz Varian Unity spectrometer. Approximately 2 mM aqueous solutions at pH 5.6 were prepared for measurement at 1°C and 5°C. Commonly used homonuclear two-dimensional spectroscopy was applied. In all experiments the acquisition time was 320 ms, corresponding to the spectral width of 6400 Hz with 2048 complex points. The number of increments for the indirect dimension was 256 in TOCSY and NOESY, but 512 in COSY. Solvent signal suppression was achieved by continuous wave presaturation during the recycling delay (1.2 s). The residual water signal was further reduced by a time domain convolution (McIntyre and Freeman, 1992). Time domain data were weighted by shifted sinebell squared for TOCSY and NOESY and sinebell for COSY in both dimensions. The result matrices were $2k \times 1k$ points.

The spin systems of the amino acids were identified according to the through-bond couplings observed in COSY and TOCSYs taken with different mixing times (70, 90, and 120 ms). A sequence-specific assignment was then pursued according to the sequential through-space interactions observed in NOESY taken with a 500-ms mixing time. However, a complete unambiguous assignment turned out to be too difficult to obtain in spite of the high magnetic field, owing to a severe resonance overlap, particularly of the α, β, and δ carbon-bound protons of the many prolines in the toxins.

Computer simulations

For molecular modeling CHARMm, Ver. 2.2 software (Brooks et al., 1983; Momany and Rone, 1992; Molecular Simulations Incorporated, 1992), with its standard parameter set and amino acid models, was used. Standard algorithms for molecular mechanics (optimization), annealing, and molecular dynamics with or without restraints were also employed. The SHAKE algorithm (van Gunsteren and Berendsen, 1977) was used to constrain bond lengths of hydrogens. A 1-fs time step was employed in all simulations. The nonbonded interactions were truncated using the SWITCH function (Molecular Simulations Incorporated, 1992) for the van der Waals interactions and the SHIFT function (Molecular Simulations Incorporated, 1992) for the electrostatic interactions. These cut-off distances were altered in different stages of the simulations. The solvent simulations were performed in a 30-Å box, where density was set to 1 kg/liter using about 1000 TIP3P type (Jorgensen, 1982) water molecules. During simulations periodic boundary conditions were used for all three dimensions of the cube. The computations were carried out on Silicon Graphics 4D/380 workstation, a Silicon Graphics Power Onyx computer, and a Cray X-MP EA/464 supercomputer at CSC (Finnish National Supercomputer Center).

RESULTS

Effect of WTX1 at the neuromuscular junction

The left panel of Fig. 1 demonstrates the effect of WTX1 on the amplitude of end-plate potentials. In the example shown,

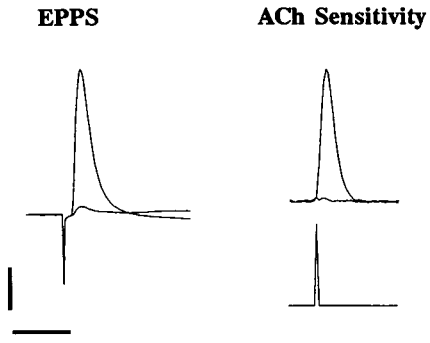

FIGURE 1 WTX1 reduces the response of the motor end plate to acetylcoline that is released from the nerve terminal or is iontophoretically applied. The large end plate potential (EPP) on the left represents the average of 50 control responses to nerve stimulation at 0.5 Hz. The smaller record is the average of 10 EPPs recorded 80–100 s after application of 1 μM WTX1. EPPs were recrded at the same end-plate in the crush fiber mouse soleus nerve-muscle preparation. The right half of the figure shows the average response of the motor end-plate of the triangularis sterni nerve-muscle preparation to 10 iontophoretically applied acetylcholine pulses of 2 ms duration and 40 nA amplitude (*lower right panel*). The larger and smaller responses shown in the upper right represent the control responses (large EPP) and that after the application of 1 μM WTX1. Calibration bars: vertical, 2 mV and 20 nA; horizontal, 10 ms for EPPs and 24 ms for acetylcholine sensitivity recordings.

EPP amplitude declined 93% within 1.5 min after the application of 1 μM WTX1. For seven neuromuscular junctions, 1 μM WTX1 reduced mean EPP amplitude by 82 ± 5%. Because this effect of WTX1 could be due to either pre- or postsynaptic action, the sensitivity of the motor end plate to iontophoretically applied acetylcholine was measured. The right panel of Fig. 1 demonstrates the ability of WTX1 to decrease the end-plate sensitivity to acetylcholine. For the fiber shown, the acetylcholine response declined 95% within 2 min after the application of 1 μM WTX1. For seven separate motor end plates, 1 μM WTX1 reduced the sensitivity of iontophoretically applied acetylcholine by 77 ± 4%.

Disulfide bond formation

The critical role of disulfide bond formation in determining the activity of WTX1 (Schmidt et al., 1992) led us to make a number of single amino acid substitutions. Based on initial analyses, position 10 was found to be a particularly rigid part of the loop defined by the disulfide bond. Therefore, two substitutions were done, Gly10 and Phe10. The former would produce greater flexibility at this position, whereas the latter amino acid has characteristics similar to, but not mimicking, those of the native WTX1 (His) or WTX2 (Tyr).

Because the Gly10 and Phe10 analogs were obtained commercially, it was necessary to verify the purity and sequence of both peptides. HPLC analysis provided a convenient method for determining homogeneity of peptide solutions and identifying some differences between peptides by measuring retention time in the HPLC column. When subjected to HPLC analysis Gly10 appeared nonhomogeneous (Fig. 2 *a*). The main peak had a retention time of

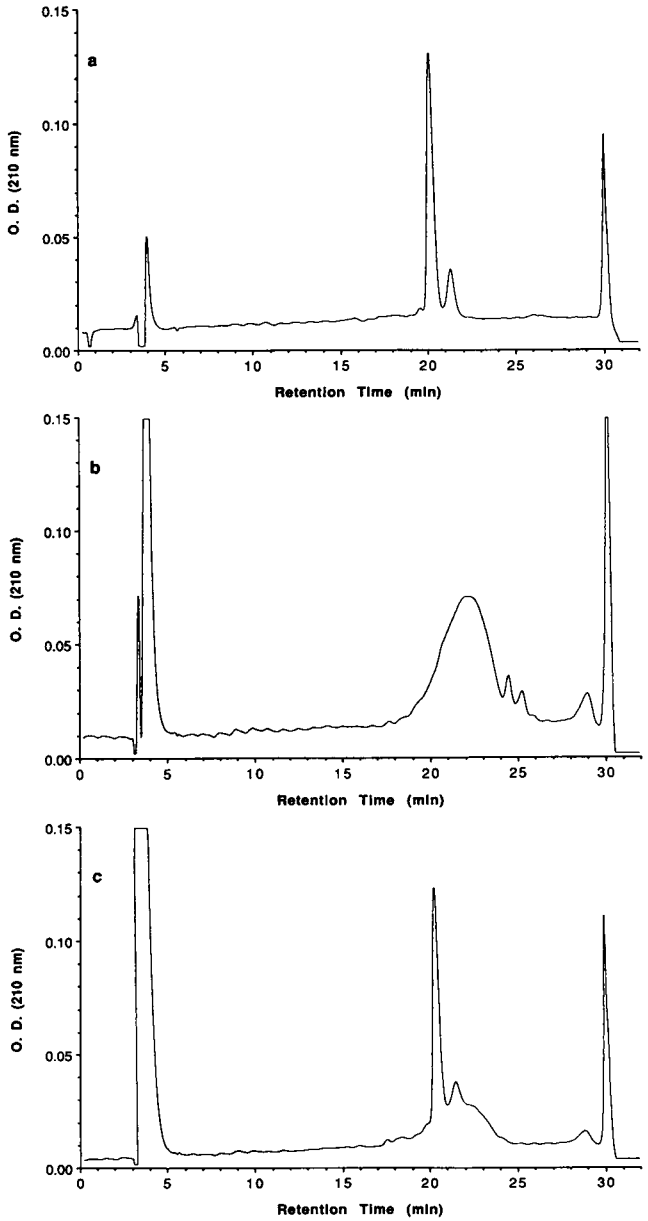

FIGURE 2 Oxidation of Gly10 analog. (*a*) Gly10, as synthesized, before incubation at pH 8.3. The column was first equilibrated with 21% solvent B. After sample injection, the column was held at 21% B for 2.5 min, followed by a linear gradient to 30% B at 25 min. The column was then eluted with 100% B for 6 min. (*b*) Gly10 (1 mg/ml) after 18 h at pH 8.3. The gradient was the same as in *a*. (*c*) Gly10 (0.05 mg/ml) after 18 h at pH 8.3. The gradient was the same as in *a*. Peaks at 4 and 30 min were due to buffer components or solvent refractive index changes, which are seen as absorption peaks when measured at 210 nm.

21.76 min, and the smaller peak had a retention time of 22.8 min. Peaks at 4 and 30 min were due to buffer components or solvent refractive index changes, which are seen as absorption peaks when measured at 210 nm. The ratio of peak areas as determined by integration was about 4 to 1. However, only the stipulated sequence was found on amino acid sequencing, and the manufacturer's chromatogram showed only one peak. A similar situation was found for the Phe10 analog.

It is well known that pure peptides and proteins can sometimes exhibit multiple peaks on various types of chromatography, because of such factors as different conformations, selective binding of ions, etc. (see Francis et al., 1991). For example, we found that WTX1, whether isolated from venom or chemically synthesized, showed a persistent small shoulder on the front of the main peak on reverse-phase chromatography (Weinstein et al., 1991; Schmidt et al., 1992). Upon rechromatography, fractions exhibited this same shape whether collected from the front or the rear of the peak. Thus, the shoulder is not likely to be a contaminant but is probably due to different degrees of histidine protonation, binding to trifluoroacetate, or different conformations about the many proline bonds.

For Gly10 and Phe10, the manufacturer's reverse-phase chromatograms showed single peaks. The differences observed may be due to different gradients used in generating these traces. Unlike the steep gradients used by many peptide manufacturers, which do not resolve closely eluting peaks, the chromatograms shown here were done with relatively shallow gradients. We cannot entirely rule out the possibility that changes such as partial oxidation or rotation about proline bonds took place during storage. However, we are confident that the peptides used in this study were pure and the presence of asymmetrical peaks and/or additional peaks on the chromatograms was not due to contaminents, but to one or more of the factors described above.

Lethality measurements indicated that the Gly10 analog was nontoxic (mouse i.p. $LD_{50} > 22$ mg/kg). In contrast to WTXI, which oxidizes completely to a single product with a intramolecular disulfide bond, the Gly10 analog did not form the intramolecular disulfide bond after incubation at alkaline pH. Instead, after 18 h, there was a broad, irregular later-eluting main peak, plus two smaller peaks fused with it (Fig. 2 *b*). It was necessary to determine if this was a concentraton-dependent phenomenon because oxidation of reduced, synthetic WTXI at concentrations higher than 1 mg/ml led to formation of biologically inactive products with retention times longer than the parent molecule (Schmidt et al., 1992). This inactivity resulted from the formation of intermolecular disulfide bonds. It was possible that a similar concentration-dependent effect was occurring with the Gly10 analog, even at 1 mg/ml. Therefore, we tried oxidizing Gly10 at a lower concentration, to see if this would lead to a single product, but it did not (Fig. 2 *c*). However, we did find that oxidation of Gly10 was much slower at 0.05 mg/ml than at 1 mg/ml. In contrast, the oxidation rate of WTX1 was not concentration dependent. These data imply that the Gly10 preferentially forms an intermolecular disulfide bond and explain why the Gly10 is nontoxic.

Lethality determinations of the Phe10 analog showed that incubation at pH = 8.3 for 6 h produced a LD_{50} value of 18 mg/kg. When the same concentration of peptide was allowed to oxidize at pH = 8.3 for 18 h, the LD_{50} was 5 mg/kg. These results suggested that, unlike the Gly10 analog, Phe10 can form the crucial intramolecular disulfide bond, but at an extremely slow rate.

To examine further this hypothesis, Phe10 was subjected to HPLC analysis. Before oxidation, Phe10 gave an asymmetrical peak on HPLC (Fig. 3 *a*), suggesting that the

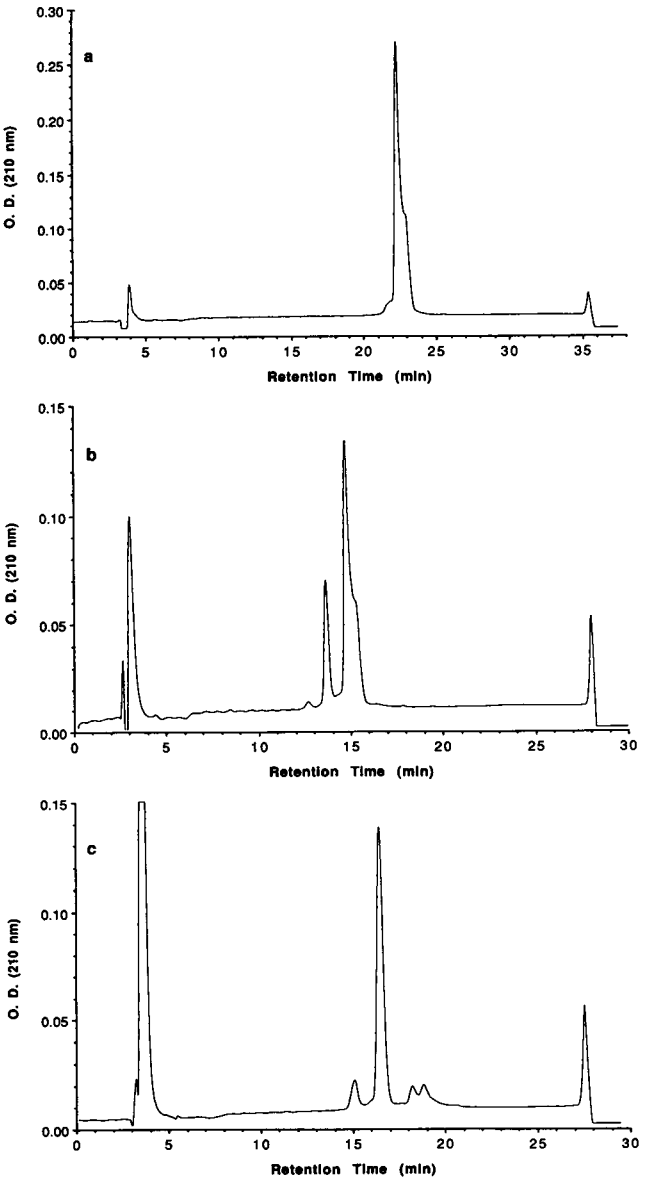

FIGURE 3 Oxidation of Phe10 analog. (*a*) Phe10, as synthesized, before incubation at pH 8.3. The column was first equilibrated with 18% solvent B. After sample injection, the column was held at 18% B for 2.5 min, followed by a linear gradient to 45% B at 31 min. The column was then eluted with 100% B for 6 min. (*b*) Phe10 (1 mg/ml) after 7 h at pH 8.3. In this case, the column was first equilibrated with 23% solvent B. After sample injection, the column was held at 23% B for 2.5 min, followed by a linear gradient to 45% B at 31 min. The column was then eluted with 100% B for 6 min. (*c*) Phe10 (1 mg/ml) after 51 h at pH 8.3. The column was first equilibrated with 24% solvent B. After sample injection, the column was held at 24% B for 2.5 min, followed by a linear gradient to 38% B at 31 min. The column was then eluted with 100% B for 6 min. Peaks at 4 and 30 min were due to buffer components or solvent refractive index changes, which are seen as absorption peaks when measured at 210 nm.

preparation was not homogeneous. However, only the stipulated sequence of the peptide was found on amino acid sequencing. Furthermore, an HPLC chromatogram of the peptide supplied by the manufacturer showed only one, symmetrical peak. These findings suggested that the Phe10 might have undergone chemical change(s) during storage. However, the discrepancies observed for the Phe10 analog can also be explained in the same way as described for the Gly10 analog above. Regardless, after incubation at alkaline pH, Phe10 oxidized to a single, symmetrical peak with a lower retention time than the parent molecule, although oxidation took place at a much slower rate compared to WTX1. After 7 h at pH 8.3, approximately 22% conversion of Phe10 to the disulfide-bonded form was found (Fig. 3 *b*). Oxidation was essentially complete in 51 h (Fig. 3 *c*). A comparison of the oxidation rates of WTX1 and Phe10 is shown in Fig. 4.

The percentage conversion to the disulfide form was measured by integration of peak areas on HPLC. At the indicated times, the reaction was stopped by adjusting the pH to 2.0–3.0 with TFA. That this step does indeed stop the oxidation is demonstrated by the fact that after acidification, the chromatographic patterns of the individual samples remain constant, even after several months of storage at 4°C. These data support the notion that, like WTX1 and WTX2, the Phe10 analog preferentially forms the intramolecular disulfide bond, but at a rate approximately an order of magnitude slower.

NMR analysis

The 2D spectra COSY, TOCSY, and NOESY were obtained for WTX1 and Gly10. Most of the protons had resonance frequencies that were close to their average random coil values (Wüthrich, 1988). This often caused an overlapping of two or more peaks, which made the NOE spectra difficult to assign. A total of 224 NOE peaks were assigned for both peptides. The peaks were first assigned from the spectra of Gly10, but later analysis showed that all of the assigned peaks could also be found in the spectra of WTX1 (Fig. 5). The NOE peaks were mainly produced by intraresidual or sequential proton interactions and thus gave little structural information. For all prolines in the tail regions (Pro4, 8, 17, 19, and 21) a close contact between the proline δ-protons and α-proton of the proceeding amino acid was detected, which means that the prolines were *trans*-oriented. The lack of longer-range interactions and average random coil values of resonance frequencies clearly implied an extended overall structure.

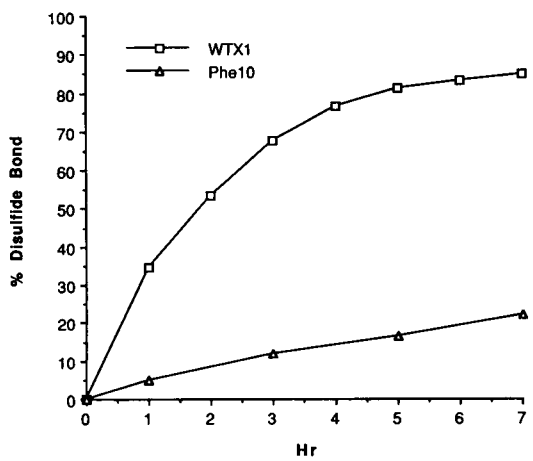

FIGURE 4 Time course of disulfide bond formation in WTX1 and Phe10 analog at pH 8.3.

Only a few exceptions to the extended structure were discovered. A weak contact between the main-chain amide protons of Asp5 and Leu6 was detected, which could imply a tendency for a helical structure in this region. Nonsequential interactions were also found between δ-protons of Tyr15 and the α-proton of Pro17. Another interesting feature was that multiple conformations were found for the NH proton of Ile16. This shows that the peptide does not have a single fixed structure in aqueous solution.

In the loop region, strong frequency overlap of proline protons, in particular H_β and H_γ, made it difficult to assign unambiguously the Pro11 and Pro12 NOE peaks. The assigned peaks between Pro11 Hδ and Pro12 Hα nevertheless indicated that the bond between the two sequential prolines was *trans*-oriented. However, the HB-HB intercysteine cross-peak also could not be unambiguously assigned.

To make sure that the internal disulfide bond existed in the examined peptide, a simple experiment was carried out. First, a 1D NMR spectrum was measured from WTX1 in solution. Then dithiotreitol in twofold molar excess with respect to the peptide was added to reduce the disulfide bond, and a new 1D spectrum was subsequently acquired (Fig. 6). The two spectra were different. A detailed examination revealed changes of resonance frequencies for protons adjacent to the disulfide bond. In the disulfide-bonded WTX1 spectrum, the resonance lines of HN protons of cysteines were located at 8.95 ppm and 8.84 ppm, respectively, at the most high-field region of the spectrum. This is a sign of a chemical environment different from that of most of the other residues. After breaking the disulfide bond, the peaks were shifted downfield, closer to random coil values of NH resonance frequencies. This implied that in the chemical environment characteristic of the disulfide bridge, a closed loop, had disappeared.

Chemical shift changes were observed for protons of the aromatic rings of His10 and His14 and for α- and δ-protons, presumably from Pro11 and Pro12. For protons of the tails of the peptide, such as N-protons of Asp5, Lys20, or Arg22, no clear shifting was observed, as expected. These results proved that the internal disulfide bond existed in the studied WTX1 molecules and that it brought structural integrity to the loop region.

Circular dichroism

The CD spectrum of WTX3 in TFE shows a minimum of 208 nm and an inflection point at about 222 nm. When the

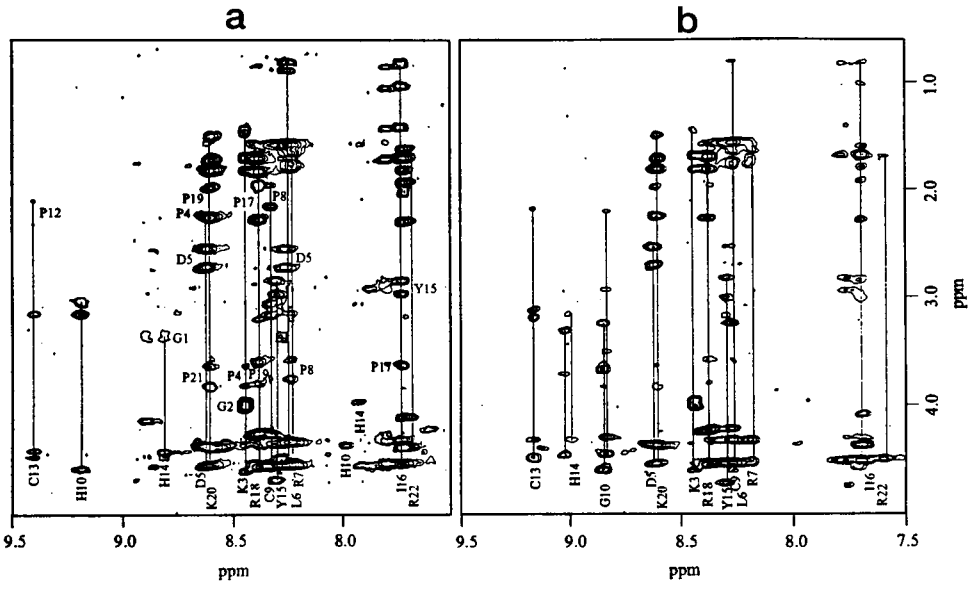

FIGURE 5 A part of the 2-dimensional NOE spectra. HN resonances are shown by vertical lines and marked with labels; horizontal labels indicate sequential assignments. (*a*) WTX1; (*b*) Gly10.

solution was diluted with water, the minimum moved to the lower wavelengths of 204 and 202 nm for TFE:H_2O (4:1) and TFE:H_2O (10:1), respectively. Furthermore, the inflection point disappeared and the spectrum became convex in that region. We interpret the spectrum in TFE to indicate a helical content in WTX3, because the wavelengths of the minimum and the inflection point correspond approximately with minima characteristics of the α-helix. Qualitatively this could result in broadening of the first minimum at about 230 nm to an inflection point and to deepening of the second minimum. Furthermore, the amount of random coil content is apparently increased as water is added because the minimum shifted to lower wavelengths and the CD spectrum does not reach a positive amplitude typical of helical or β-sheet structures. However, mM solutions of WTX3 in TFE and TFE:H_2O (10:1) were not stable, forming aggregates over several days. This was also apparent in NMR spectra, resulting in broad lines and a poor signal-to-noise ratio. Therefore, structural determination in TFE environments was not feasible. This problem may be solved by analysis of the peptide structure in DMSO.

Peptide modeling: conformation of WTX1 in solution

Computer simulations and a search for conformations were started with extended or partly helical conformations in the presence of the disulfide bond. Vacuum simulations without restraints were found inappropriate for the case of polar solvent, although they could be relevant for a less polar environment such as TFE. This is due to the overemphasis on the long-range electrostatic interactions and hydrogen bond formation within and between the C- and N-terminal

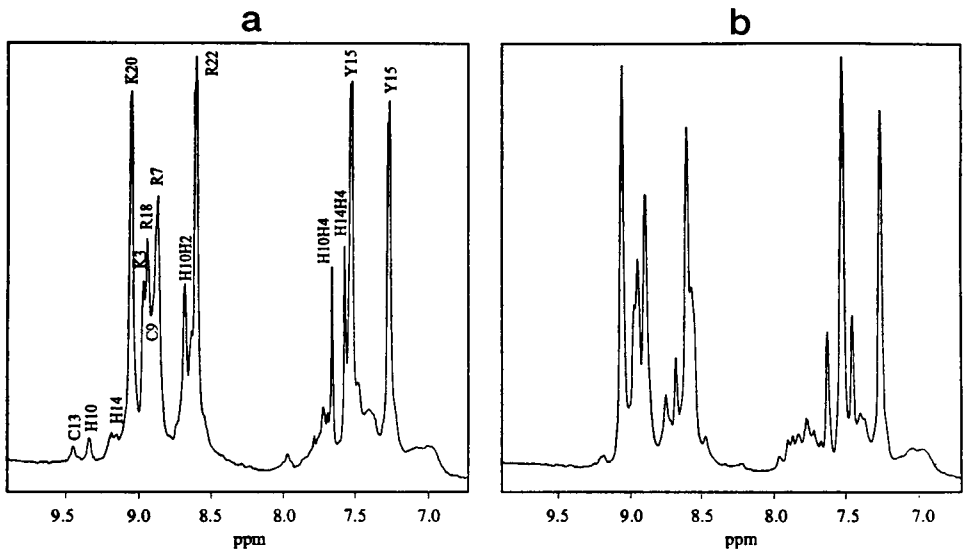

FIGURE 6 1-D spectra of WTX1 from the NH region. (*a*) Spectra for active peptide. (*b*) Spectra after the disulfide bond has been broken using dithiothreitol.

regions of the peptide. These interactions favored more coiled conformations, in contradiction to the interpretation of the CD and NOE spectra in water solution, but in better agreement with the CD spectrum in TFE. In vacuum simulations, a stable helix-like conformation was found for the N-terminus. However, water as a solvent obviously effectively screens long-range electrostatic interactions.

When the vacuum conformation was placed into a water environment, the strong intramolecular interactions in the peptide were reduced. Even though the peptide gradually started to unfold and some of the intramolecular hydrogen bonds were replaced with hydrogen bonds to surrounding water molecules, the 32-ps simulation time used was far too short to reach an extended peptide conformation where all vacuum induced interactions would have disappeared. One could speculate, however, that similar but opposite conformational changes take place when the peptide moves from a polar to a less polar environment, like that of the cell membrane.

The first available NMR (NOE) data were used to set restraints on the interatomic distances in the regions outside the loop defined by the disulfide bond. These restraints were divided into three categories according to the intensity of the corresponding peak in NOE spectra. Restraints obtained from the strongest peaks allowed the atom distance to vary between 1.8 Å and 3.0 Å without an energy penalty. For smaller NOE peaks, limits from 1.8 Å to 4.0 Å and from 1.8 Å to 5.0 Å were used. Because only one NH-NH cross-peak, between Asp5 and Leu6, was detected in NOE spectra, a group of extra restraints was used to keep the other tail region NH atoms at least 4.0 Å apart. The NMR data were actually measured from a Gly10 analog but were also found to be applicable for the WTX1 at the tail regions beyond the disulfide bond.

The search for conformations in aqueous solution was started with the vacuum conformation that had the least violations to the NOE restraints. After 10 ps heating and 20 ps equilibration, the peptide was simulated for 35 ps in 310 K without NOE restraints. During the simulation, the peptide experienced some conformational changes, but the overall structure remained the same. The RMS fluctuations of angles and dihedral angles between sequential α-carbons $C_{\alpha i-1}$-$C_{\alpha i}$-$C_{\alpha i+1}$ (Fig. 7) showed that His10 seemed to be in a more rigid position than the rest of the peptide. The large RMS fluctuations at positions 8, 11, and 13 seen in Fig. 8 are artifacts, caused by the gradual drift of about 20°, which occurred during the simulations. Nevertheless, at the end of the simulation only angle $C_{\alpha 7}$-$C_{\alpha 8}$-$C_{\alpha 9}$ still had a clear tendency to drift while the other angles seemed to have reached the equilibrium.

The average conformation of the last 15 ps of the simulation was computed to study the conformational family in water solution. In a phi/psi plot (Fig. 9), most of the residues of the average structure are located in the extended or β-sheet region. The only exceptions are His10, Pro19, and Lys20, which were in the α-helix regions. The disulfide bond is the right-handed type. The C_β-S_γ-S_γ-C_β dihedral

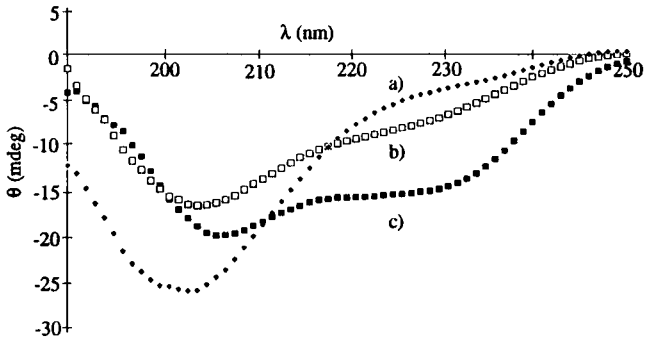

FIGURE 7 Circular dichoism spectra of WTX3 (*a*) TFE (trifluoroethanol):H_2O (4:1); (*b*) TFE:H_2O (10:1); (*c*) TFE.

angle is 83°, near the ideal 90°. The final solution conformation still has four violations (>0.3 Å) of the restraints. The largest violations are found between Tyr15 and Pro17 and are caused by the rotation of the side chain of Tyr15.

If the simulated conformation were the optimum one with respect to the NMR data, one might expect that no violations of the restraints would remain. The fact that several violations (<1.0 Å) still remained may imply that the conformation could be further refined or the restraints are too tight. The NOE restraints are probably too tight because they were obtained from an ensemble of conformations, and consequently, any single structure cannot simultaneously satisfy all of these restraints. In the loop region, less experimental information was available, for reasons described above. However, the conformational free space of the backbone is strongly reduced because of the disulfide bond and the two prolines. Because no large violations of the restraints appeared for the main-chain atoms, the overall shape of the conformation can be expected to represent the actual conformation family of active WTX1 in solution, as shown in Fig. 10.

The NOE spectra of the Gly10 analog were very similar to those of WTX1, and particularly for the tail region (1–9 and 14–22) protons, no significant differences were found. Most of the differences were detected in the loop region due to the different amino acid in position 10 and possible multiple conformations for the Gly10 analog.

Substitution of His10 with Gly10 was found to produce an analogous molecule that favors intermolecular instead of intramolecular disulfide bonds. To determine what structural features lead to this difference, the effect of breaking the disulfide bond and substituting His10 with Gly10 was simulated. Shortened peptide models, which included only 11 residues Leu6–Ile16, were used. This was done to save computational resources, because solvent simulations of unfolded full peptides would have required a significantly larger water box. The NMR data also showed that the structure of the tail parts of the peptide were not affected by disulfide bond formation, and thus it was expected that those parts of the peptides do not substantially affect bond formation. In the shortened peptide computer models, the disulfide bond was not initially formed, cystines were re-

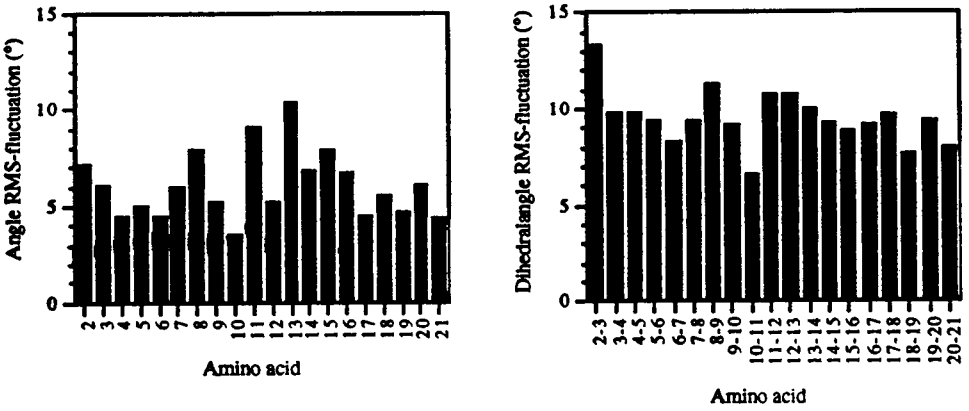

FIGURE 8 The RMS fluctuations of angles and dihedral angles between sequential α-carbons of the peptide backbone during the 35-ps solvent simulation. The numbering at the horizontal axis refers to the one or two centermost C_α atoms of the angle or the dihedral angle.

placed by cysteines, and terminal amino and carbonyl groups were replaced with methyl groups to avoid disturbing the effects of polar terminal groups.

The simulation was carried out in three phases. First, the shortened peptides were simulated in water solution for 30 ps. The initial conformation for the selected residues (Leu6 to Ile16) was obtained from the average structure of the WTX1 simulation. As no restraints were used, the peptide conformations were already slightly altered during heating and equilibration. During the actual simulation the conformations had no tendency to open up toward more extended structure, even though the disulfide bond was not constraining the loop region. In WTX1, no close contacts between the tails occurred, but in Gly10 a few hydrogen bonds between Arg7 and Ile16 were formed during the simulation. Distances between the cysteines did not change much compared to the native WTX1. In both shortened peptides the S-S distance was increased from 2.0 Å to about 4.5 Å. The distances between $C_{\alpha 9}$ and $C_{\alpha 13}$ had increased from 5.8 to 6.5 Å in the shortened WTX1 peptide, but for the shortened Gly10, the distance was decreased to 5.4 Å. Both shortened peptide conformations were folded in a manner that one might expect to imply disulfide bond formation. For example, if we compare these results to *ab initio* calculations for the 1,3-propanedithiol (Honda et al., 1989), where the optimum distance between nonbonded sulfur atoms was found to be about 4.2 Å, the distances between the cysteines and the χ-angles are, in our case, quite similar.

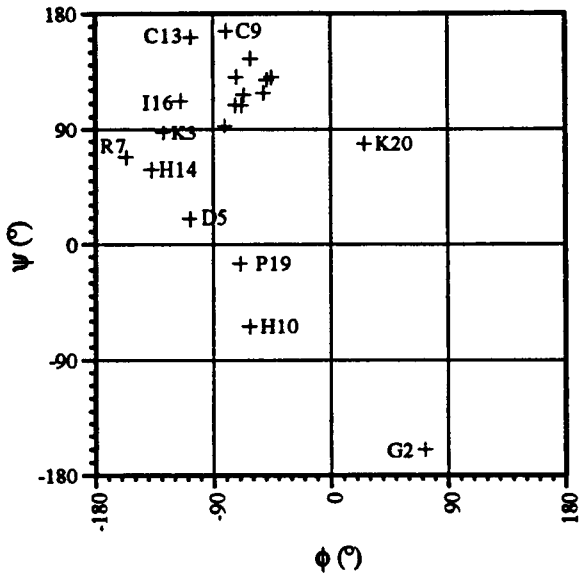

FIGURE 9 Phi/psi plot (Ramachandran et al., 1963) of the average structure of WTX1. Only the amino acids located outside the proline region are labeled.

The comparison of the two shortened conformations clearly indicated that, near the native-like conformation, there are no sterical hindrances or potential barriers, which would make the formation of intramolecular disulfide bond less favorable for Gly10. In fact, the increased flexibility at position Gly10 let the backbone bend even more, so that average distance of C_β and C_α atoms of the two cysteines was about 1 Å shorter in Gly10 than in WTX1.

In the second phase, the two peptide models were forced to unfold in vacuum conditions using minimization with a set of gradually increasing distance restraints (Fig. 11). The main restraint, which was used to cause the unfolding, was set between Leu6 Ca and Ile16 Ca. Two additional restraints (Arg7 Cζ–Ile16 Cα and Arg7 Cζ–Pro11 Cα) were used to prevent the vacuum-induced hydrogen bonds of the arginine side chain during the opening.

In the beginning of the unfolding process the changes occurred mainly in the dihedral angles, and total energies of the molecules increased slowly. When the Arg7 Cζ–Ile16 Cα distance had reached 30 Å, bond angles and lengths also started to change and the potential energy began to increase more rapidly. This was interpreted as a sign of overstrained structure and thus the conformations obtained using a 29.5 Å restraint value were selected to present the unfolded peptides.

In the third phase, unfolded conformations of the two peptides were embedded back to a 30-Å water box. The peptides were first simulated for 30 ps with the unfolding restraints, and then for 40 ps without any restraints. In their unfolded state the two fragments were still quite similar, but after removing restraints the fragments started to fold in different ways. The loop region of the shortened WTX1 had a clear tendency to return to the native, loop-like structure

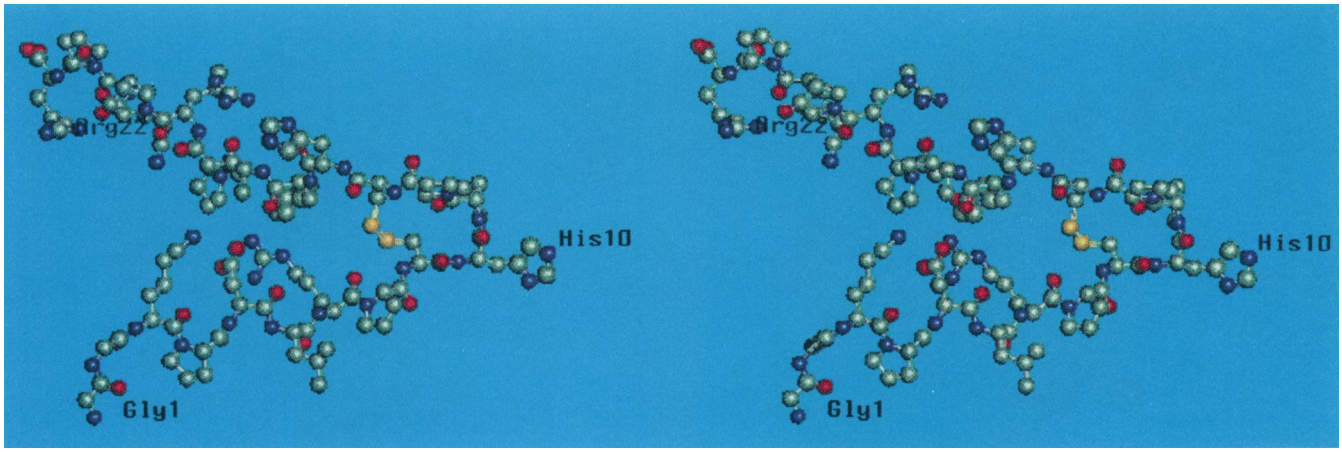

FIGURE 10 The average structure (in stereo) of the last 15 ps of the WTX1 in water solution simulation. Only the heavy atoms of the peptide are shown.

(Fig 12 *a*). During the 40-ps simulation the distance between Leu6 Ca and Ile11 Ca decreased from 29 Å to 22 Å, and the cysteine side chains started to approach each other. The Gly10 substitution, on the other hand, increased the flexibility of the main chain at the loop region. Consequently, folding of the Gly10 analog was slower and did not approach native-like loop structure, but allowed the side chain of Cys9 to bend outward, away from the side chain of Cys13 (Fig. 12 *b*).

Even though the simulations were very short and were not carried through to equilibrium, they give some idea about the effect of the Gly10 substitution. Substitution seems to increase the flexibility of the loop, especially for the ψ_{10} angle, which allows the Gly10 analog to fold differently compared to the native WTX1. This obviously allows easier formation of the intermolecular disulfide bond. The fact that the shortened model of the WTX1 quite rapidly starts approaching the disulfide bond-forming structure is probably caused by the rigid unfolding method. The simulation also suggests that the tail parts are not necessary for the folding of the loop. The sequence Cys-His-Pro-Pro-Cys favors a loop-like structure, which may be a general feature of this type of sequence.

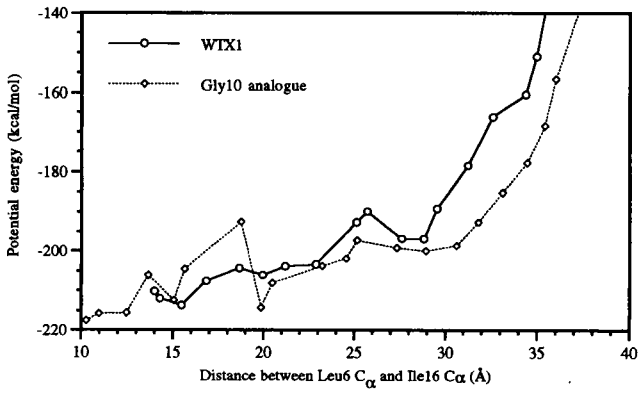

FIGURE 11 Development of potential energy of the peptide fragments during unfolding. In the beginning the distances between Arg7 C_α and Ile16 C_α were 10.7 Å in WTX1 and 9.8 Å in the Gly10 analog. The lower limit of the restraint was increased from the starting value 1.5 Å at a time after which the structures were minimized. The upper limit of the restraint was all the time hold 0.1 Å higher than the lower limit. The first values of the plot were obtained after the first unfolding cycle.

DISCUSSION

The pharmacological data presented confirm an earlier report (Aiken et al., 1992) that WTX1 suppresses end-plate potentials. However, that study suggested that this effect could be due to either a direct action on the end plate or an indirect action on the motor nerve terminal. Because WTX1 blocked the response to iontophoreticaly applied acetylcholine at concentrations comparable to that required to block EPPs, we suggest that the primary action of WTX1 at the mature neuromuscular junction is to block the nicotinic acetylcholine receptor. This contention is supported by the observation that WTX1 competitively inhibits (IC_{50} = 3.5 μM) the binding of α-bungarotoxin to the acetylcholine receptor (McArdle et al., manuscript submitted for publication). Furthermore, WTX1 does not affect the time course of end-plate current decay, suggesting an absence of nonspecific effects on the ion channel (Aiken et al., 1992).

The NMR results indicate that, in an aqueous environment, WTX1 has extended and flexible "tail" regions on either side of the short, rigid disulfide-bonded loop. Based on experiments using circular dichroism, these flexible regions will show a different 3-dimensional structure when the peptide is placed in a less polar environment. Undoubtedly, this ability to undergo structural rearrangement when presented with different environmental conditions could contribute to the ability of WTX1 to interact effectively with multiple receptor sites. This does not exclude the possibility that similarities exist in the binding sites among different receptors, especially those that may belong to the same superfamily of proteins. However, as mentioned earlier, there is some selectivity in these multiple sites of action, and the differences may prove valuable in probing

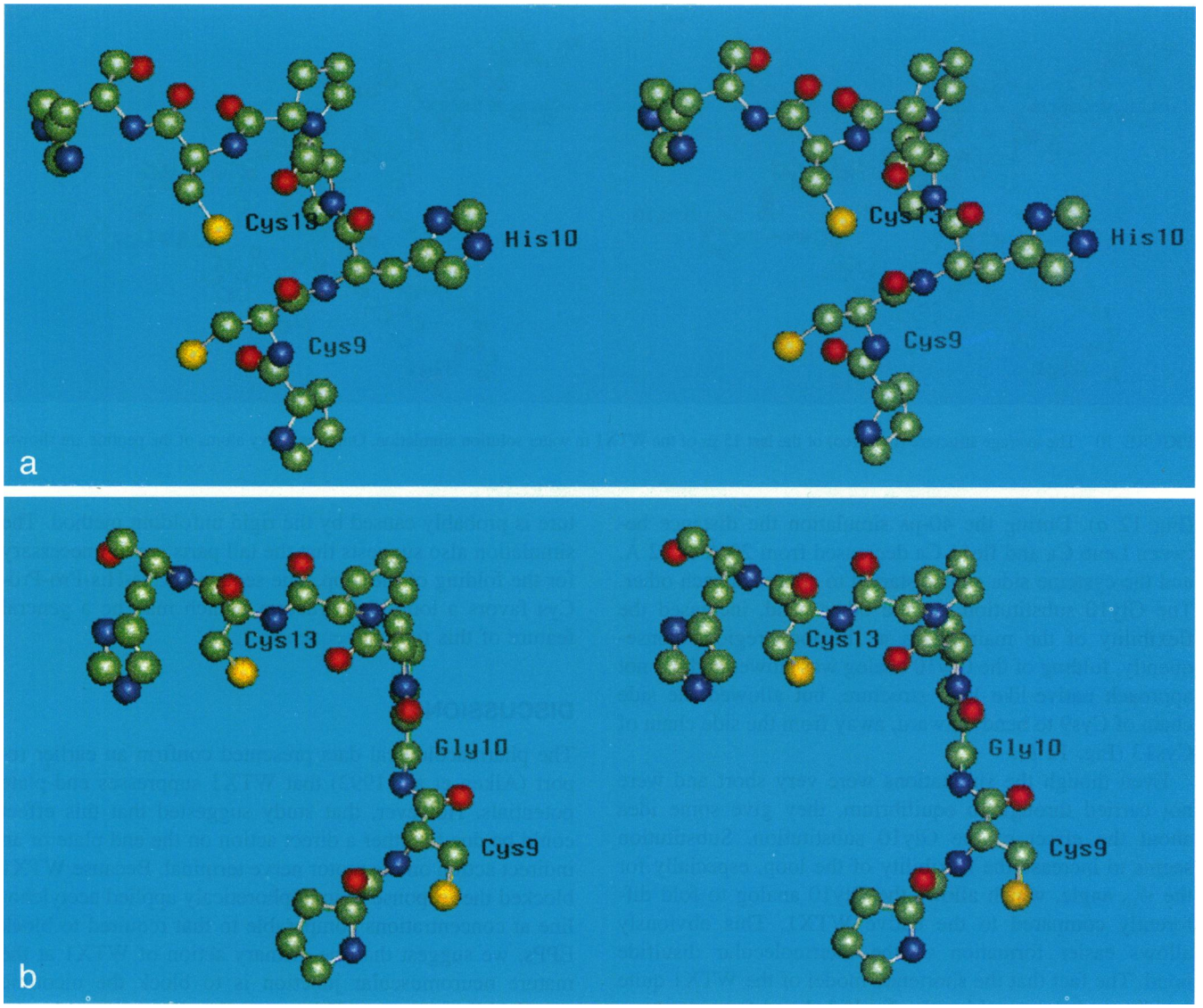

FIGURE 12 Loop region structures of WTX1 (*a*) and Gly10 analog (*b*) fragments after refolding simulations. The figures present an average conformation of the last 5 ps of the 40-ps refolding simulation in water. Only heavy atoms of region Pro8-His14 are shown.

the receptor sites and the effects of WTX1 on both voltage- and ligand-gated channels. In this regard, the ability of WTX1 to enhance $GABA_A$- and glycine-activated, but not kainate-activated channels is particularly interesting (Ye and McArdle, 1995), given the fact that WTX1 clearly blocks acetylcholine-gated channels at the neuromuscular junction (Aiken et al., 1992; McArdle et al., 1995). It is also possible that in some cases the agonist or antagonist activity may be concentration-dependent.

Single amino acid substitutions at position 10 produced significant differences in structures and activities compared to the native WTX1 peptide. The computer simulations also suggest that position 10 is important from a structural point of view. In native WTX1 the His residue is clearly the most rigid part of the structure which, together with the nearby prolines, experiences only minor changes during different simulation steps.

Substituting Gly for His at position 10 produced a non-toxic analog that preferentially formed an intermolecular rather than an intramolecular disulfide bond. The NMR restrained simulations provided some hints for why the Gly10 analog preferably forms the intermolecular disulfide bond. From the 3-dimensional perspective, the Gly in position 10 allows the peptide to bend and fluctuate more, which decreases the probability of intramolecular disulfide bond formation. On the other hand, the simulations suggest that the Gly10 substitution can also affect the folding in a way that favors the formation of the intermolecular disulfide bond. One possibility could also be the *cis-trans* isomeria in position 10, where the potential energy of the *cis* isomer seems to be close to the normal *trans* configuration. It is interesting to note that WTX1 in its reduced form reverts to its lethal oxidized, disulfide-bonded structure even after injection into mice (Weinstein et al., 1991). Thus, the loop

structure of WTX1 seems to be optimized for disulfide bond formation and, consequently, ensures its high toxicity.

After incubation at pH 8.3, most of the Phe10 analog rearranged to form a product that gave a faster-eluting, relatively symmetrical, and sulfhydryl-negative peak on HPLC. These observations suggest that oxidation of Phe10 led to the formation of a single intramolecular disulfide bond. However, the rate of disulfide bond formation in Phe10 is very slow compared to WTXI or WTX2. This is particularly relevant in regard to WTX2, which has Tyr at position 10. That a difference of a single hydroxyl group should result in such a profound change in disulfide bond formation raises some interesting questions. From the modeling point of view WTX2 and the Phe10 analog are quite similar and the small electrostatic difference between Tyr and Phe would probably produce only minor effects in a computer simulation. Significant information might be obtained by calculating the free energy changes between the folded and unfolded conformations of the peptides. This information could be compared with the rate constants of disulfide bond formation and thus provide a basis of comparison between the biochemical and the structural results.

Even though the NMR spectroscopy and the simulations gave some information about the structure, folding, and disulfide bond formation, the binding mechanism of the peptide still remains unclear. The studies of structure-activity relations would clearly require that the receptors be taken into account, in both structural determinations and dynamic simulations.

The authors acknowledge research support from the Foundation of Neste, Inc. (A. A.), the Ella and George Ehrnrooth Foundation (A. A.), and National Institutes of Health grant NS 31040 (J. J. M.)

REFERENCES

Aiken, S. P., L. C. Sellin, J. J. Schmidt, S. A. Weinstein, and J. J. McArdle. 1992. A novel peptide toxin from *Trimeresurus wagleri* acts pre- and post-synaptically to block transmission at the rat neuromuscular junction. *Pharmacol. Toxicol.* 70:459–462.

Argentieri, T., S. P. Aiken, S. Laxminarayan, and J. J. McArdle. 1992. Physiology of regenerating neuromuscular junctions in the rat, and the effects of 2,3-butanedione monoxime. *Pflügers Arch. Eur. J. Physiol.* 421:256–261.

Brattstrom, B. H. 1964. Evolution of the pit vipers. *Trans. San Diego Soc. Nat. Hist.* 13:185–268.

Brooks, B. R., R. E. Bruccoleri, B. D. Olafson, D. J. States, S. Swaminathan, and M. Karplus. 1983. CHARMm: a program for macromolecular energy, minimization, and dynamic calculations. *J. Comput. Chem.* 4:187–217.

Francis, B., T. R. John, C. Seebart, and I. I. Kaiser. 1991. New toxins from the venom of the common tiger snake (*Notechis scutatus*). *Toxicon.* 29:85–96.

Honda, M., and M. Tajima. 1990. The change in atomic distance between sulphur atoms on the reduction of disulphide to dithiol. *J. Mol. Struct. Theochem.* 204:247–252.

Hyvönen, M., K. Mattila, T. T. Rantala, and L. C. Sellin. 1994. Molecular modelling of a channel-blocking peptide from *Trimeresurus wagleri*. *Biophys. J.* 66:A63.

Jorgensen, W. L. 1982. Revised TIPS for simulations of liquid water and aqueous solutions. *J. Chem. Phys.* 77:4156–4163.

Leviton, A. E. 1964. Contributions to a review of Philippine snakes. V. The snakes of the genus *Trimeresurus*. *Philipp. J. Sci.* 93:251–276.

Mattila, K., A. Annila, J. J. Schmidt, M. Hyvönen, T. Kivistö, T. T. Rantala, J. J. McArdle, and L. C. Sellin. 1995. Factors affecting folding and disulfide bond formation of a small bioactive peptide. *Biophys. J.* 68:A325.

McArdle, J. J. 1975. Complex end plate potentials at the regenerating neuromuscular junction of the rat. *Exp. Neurol.* 37:629–638.

McArdle, J. J., D. Angaut-Petit, A. Mallart, R. Bournaud, L. Faille, and J. L. Brigant. 1981. Advantages of the triangularis sterni muscle of the mouse for investigation of presynaptic phenomena. *J. Neurosci. Methods.* 4:109–115.

McArdle, J. J., J. J. Schmidt, S. A. Weinstein, and L. C. Sellin. 1995. Wagler toxin I blocks the nicotinic acetylcholine receptor. *Biophys. J.* 68:A327.

McArdle, J. J., Y.-F. Xiao, S. P. Aiken, L. C. Sellin, J. J. Schmidt, and S. A. Weinstein. 1992. A novel peptide neurotoxin selectively blocks myocardial L-type calcium current. *Neurosci. Soc.* 18:969.

McIntyre, L., and R. Freeman. 1992. Accurate coupling-constants from 2-dimensional correlation spectra by J-deconvolution. *J. Magn. Reson. Imaging.* 96:425–431.

Molecular Simulations Incorporated. 1992. CHARMm Ver. 2.2. Molecular Simulations Incorporated, Burlington, MA.

Momany, F. A., and R. Rone. 1992. Validation of the general purpose QUANTA/CHARMm force field. *J. Comput. Chem.* 13:888–900.

Ramachandran, G. N., C. Ramakrishnan, and V. Saisekharam. 1963. Stereochemistry of polypeptide chain configurations. *J. Mol. Biol.* 7:95–110.

Schmidt, J. J., S. A. Weinstein, and L. A. Smith. 1992. Molecular properties and structure-function relationships of lethal peptides from venom of Wagler's pit viper, *Trimeresurus wagleri*. *Toxicon.* 30:1027–1037.

van Gunsteren, W. F., and H. J. C. Berendsen. 1977. Algorithms for macromolecular dynamics and constraint dynamics. *Mol. Phys.* 34: 1311–27.

Weinstein, S. A., J. J. Schmidt, A. W. Bernheimer, and L. A. Smith. 1991. Characterization and amino acid sequences of two lethal peptides isolated from the venom of Wagler's pit viper, *Trimeresurus wagleri*. *Toxicon.* 29:227–237.

Wüthrich, K. 1988. NMR of Proteins and Nucleic Acids. John Wiley and Sons, New York.

Ye, J.-H., and J. J. McArdle. 1995. Enhancement of $GABA_A$ and glycine currents by wagler toxin I. *Biophys. J.* 68:A327.